BABAR-PUB-01/21
SLAC-PUB-9012

Study of *CP*-violating asymmetries in $B^0 \to \pi^+\pi^-$, $K^+\pi^-$ decays

B. Aubert,[1] D. Boutigny,[1] J.-M. Gaillard,[1] A. Hicheur,[1] Y. Karyotakis,[1] J. P. Lees,[1] P. Robbe,[1] V. Tisserand,[1] A. Palano,[2] A. Pompili,[2] G. P. Chen,[3] J. C. Chen,[3] N. D. Qi,[3] G. Rong,[3] P. Wang,[3] Y. S. Zhu,[3] G. Eigen,[4] B. Stugu,[4] G. S. Abrams,[5] A. W. Borgland,[5] A. B. Breon,[5] D. N. Brown,[5] J. Button-Shafer,[5] R. N. Cahn,[5] A. R. Clark,[5] M. S. Gill,[5] A. V. Gritsan,[5] Y. Groysman,[5] R. G. Jacobsen,[5] R. W. Kadel,[5] J. Kadyk,[5] L. T. Kerth,[5] Yu. G. Kolomensky,[5] J. F. Kral,[5] C. LeClerc,[5] M. E. Levi,[5] G. Lynch,[5] P. J. Oddone,[5] A. Perazzo,[5] M. Pripstein,[5] N. A. Roe,[5] A. Romosan,[5] M. T. Ronan,[5] V. G. Shelkov,[5] A. V. Telnov,[5] W. A. Wenzel,[5] P. G. Bright-Thomas,[6] T. J. Harrison,[6] C. M. Hawkes,[6] D. J. Knowles,[6] S. W. O'Neale,[6] R. C. Penny,[6] A. T. Watson,[6] N. K. Watson,[6] T. Deppermann,[7] K. Goetzen,[7] H. Koch,[7] M. Kunze,[7] B. Lewandowski,[7] K. Peters,[7] H. Schmuecker,[7] M. Steinke,[7] J. C. Andress,[8] N. R. Barlow,[8] W. Bhimji,[8] N. Chevalier,[8] P. J. Clark,[8] W. N. Cottingham,[8] N. Dyce,[8] B. Foster,[8] C. Mackay,[8] D. Wallom,[8] F. F. Wilson,[8] K. Abe,[9] C. Hearty,[9] T. S. Mattison,[9] J. A. McKenna,[9] D. Thiessen,[9] S. Jolly,[10] A. K. McKemey,[10] V. E. Blinov,[11] A. D. Bukin,[11] D. A. Bukin,[11] A. R. Buzykaev,[11] V. B. Golubev,[11] V. N. Ivanchenko,[11] A. A. Korol,[11] E. A. Kravchenko,[11] A. P. Onuchin,[11] A. A. Salnikov,[11] S. I. Serednyakov,[11] Yu. I. Skovpen,[11] V. I. Telnov,[11] A. N. Yushkov,[11] D. Best,[12] M. Chao,[12] A. J. Lankford,[12] M. Mandelkern,[12] S. McMahon,[12] D. P. Stoker,[12] K. Arisaka,[13] C. Buchanan,[13] S. Chun,[13] D. B. MacFarlane,[14] S. Prell,[14] Sh. Rahatlou,[14] G. Raven,[14] V. Sharma,[14] C. Campagnari,[15] B. Dahmes,[15] P. A. Hart,[15] N. Kuznetsova,[15] S. L. Levy,[15] O. Long,[15] A. Lu,[15] J. D. Richman,[15] W. Verkerke,[15] M. Witherell,[15] S. Yellin,[15] J. Beringer,[16] D. E. Dorfan,[16] A. M. Eisner,[16] A. A. Grillo,[16] M. Grothe,[16] C. A. Heusch,[16] R. P. Johnson,[16] W. S. Lockman,[16] T. Pulliam,[16] H. Sadrozinski,[16] T. Schalk,[16] R. E. Schmitz,[16] B. A. Schumm,[16] A. Seiden,[16] M. Turri,[16] W. Walkowiak,[16] D. C. Williams,[16] M. G. Wilson,[16] E. Chen,[17] G. P. Dubois-Felsmann,[17] A. Dvoretskii,[17] D. G. Hitlin,[17] S. Metzler,[17] J. Oyang,[17] F. C. Porter,[17] A. Ryd,[17] A. Samuel,[17] M. Weaver,[17] S. Yang,[17] R. Y. Zhu,[17] S. Devmal,[18] T. L. Geld,[18] S. Jayatilleke,[18] G. Mancinelli,[18] B. T. Meadows,[18] M. D. Sokoloff,[18] T. Barillari,[19] P. Bloom,[19] M. O. Dima,[19] S. Fahey,[19] W. T. Ford,[19] D. R. Johnson,[19] U. Nauenberg,[19] A. Olivas,[19] P. Rankin,[19] J. Roy,[19] S. Sen,[19] J. G. Smith,[19] W. C. van Hoek,[19] D. L. Wagner,[19] J. Blouw,[20] J. L. Harton,[20] M. Krishnamurthy,[20] A. Soffer,[20] W. H. Toki,[20] R. J. Wilson,[20] J. Zhang,[20] R. Aleksan,[21] A. de Lesquen,[21] S. Emery,[21] A. Gaidot,[21] S. F. Ganzhur,[21] P.-F. Giraud,[21] G. Hamel de Monchenault,[21] W. Kozanecki,[21] M. Langer,[21] G. W. London,[21] B. Mayer,[21] B. Serfass,[21] G. Vasseur,[21] Ch. Yèche,[21] M. Zito,[21] T. Brandt,[22] J. Brose,[22] T. Colberg,[22] M. Dickopp,[22] R. S. Dubitzky,[22] A. Hauke,[22] E. Maly,[22] R. Müller-Pfefferkorn,[22] S. Otto,[22] K. R. Schubert,[22] R. Schwierz,[22] B. Spaan,[22] L. Wilden,[22] D. Bernard,[23] G. R. Bonneaud,[23] F. Brochard,[23] J. Cohen-Tanugi,[23] S. Ferrag,[23] E. Roussot,[23] S. T'Jampens,[23] Ch. Thiebaux,[23] G. Vasileiadis,[23] M. Verderi,[23] A. Anjomshoaa,[24] R. Bernet,[24] A. Khan,[24] D. Lavin,[24] F. Muheim,[24] S. Playfer,[24] J. E. Swain,[24] J. Tinslay,[24] M. Falbo,[25] C. Borean,[26] C. Bozzi,[26] S. Dittongo,[26] L. Piemontese,[26] E. Treadwell,[27] F. Anulli,[28,*] R. Baldini-Ferroli,[28] A. Calcaterra,[28] R. de Sangro,[28] D. Falciai,[28] G. Finocchiaro,[28] P. Patteri,[28] I. M. Peruzzi,[28,*] M. Piccolo,[28] Y. Xie,[28] A. Zallo,[28] S. Bagnasco,[29] A. Buzzo,[29] R. Contri,[29] G. Crosetti,[29] M. Lo Vetere,[29] M. Macri,[29] M. R. Monge,[29] S. Passaggio,[29] F. C. Pastore,[29] C. Patrignani,[29] M. G. Pia,[29] E. Robutti,[29] A. Santroni,[29] S. Tosi,[29] M. Morii,[30] R. Bartoldus,[31] R. Hamilton,[31] U. Mallik,[31] J. Cochran,[32] H. B. Crawley,[32] P.-A. Fischer,[32] J. Lamsa,[32] W. T. Meyer,[32] E. I. Rosenberg,[32] G. Grosdidier,[33] C. Hast,[33] A. Höcker,[33] H. M. Lacker,[33] S. Laplace,[33] V. Lepeltier,[33] A. M. Lutz,[33] S. Plaszczynski,[33] M. H. Schune,[33] S. Trincaz-Duvoid,[33] G. Wormser,[33] R. M. Bionta,[34] V. Brigljević,[34] D. J. Lange,[34] M. Mugge,[34] K. van Bibber,[34] D. M. Wright,[34] M. Carroll,[35] J. R. Fry,[35] E. Gabathuler,[35] R. Gamet,[35] M. George,[35] M. Kay,[35] D. J. Payne,[35] R. J. Sloane,[35] C. Touramanis,[35] M. L. Aspinwall,[36] D. A. Bowerman,[36] P. D. Dauncey,[36] U. Egede,[36] I. Eschrich,[36] N. J. W. Gunawardane,[36] J. A. Nash,[36] P. Sanders,[36] D. Smith,[36] D. E. Azzopardi,[37] J. J. Back,[37] P. Dixon,[37] P. F. Harrison,[37] R. J. L. Potter,[37] H. W. Shorthouse,[37] P. Strother,[37] P. B. Vidal,[37] M. I. Williams,[37] G. Cowan,[38] S. George,[38] M. G. Green,[38] A. Kurup,[38] C. E. Marker,[38] P. McGrath,[38] T. R. McMahon,[38] S. Ricciardi,[38] F. Salvatore,[38] I. Scott,[38] G. Vaitsas,[38] D. Brown,[39] C. L. Davis,[39] J. Allison,[40] R. J. Barlow,[40] J. T. Boyd,[40] A. C. Forti,[40] J. Fullwood,[40] F. Jackson,[40] G. D. Lafferty,[40] N. Savvas,[40] E. T. Simopoulos,[40] J. H. Weatherall,[40]

A. Farbin,[41] A. Jawahery,[41] V. Lillard,[41] J. Olsen,[41] D. A. Roberts,[41] J. R. Schieck,[41] G. Blaylock,[42] C. Dallapiccola,[42] K. T. Flood,[42] S. S. Hertzbach,[42] R. Kofler,[42] V. G. Koptchev,[42] T. B. Moore,[42] H. Staengle,[42] S. Willocq,[42] B. Brau,[43] R. Cowan,[43] G. Sciolla,[43] F. Taylor,[43] R. K. Yamamoto,[43] M. Milek,[44] P. M. Patel,[44] F. Palombo,[45] J. M. Bauer,[46] L. Cremaldi,[46] V. Eschenburg,[46] R. Kroeger,[46] J. Reidy,[46] D. A. Sanders,[46] D. J. Summers,[46] J. P. Martin,[47] J. Y. Nief,[47] R. Seitz,[47] P. Taras,[47] V. Zacek,[47] H. Nicholson,[48] C. S. Sutton,[48] C. Cartaro,[49] N. Cavallo,[49,†] G. De Nardo,[49] F. Fabozzi,[49] C. Gatto,[49] L. Lista,[49] P. Paolucci,[49] D. Piccolo,[49] C. Sciacca,[49] J. M. LoSecco,[50] J. R. G. Alsmiller,[51] T. A. Gabriel,[51] T. Handler,[51] J. Brau,[52] R. Frey,[52] M. Iwasaki,[52] N. B. Sinev,[52] D. Strom,[52] F. Colecchia,[53] F. Dal Corso,[53] A. Dorigo,[53] F. Galeazzi,[53] M. Margoni,[53] G. Michelon,[53] M. Morandin,[53] M. Posocco,[53] M. Rotondo,[53] F. Simonetto,[53] R. Stroili,[53] E. Torassa,[53] C. Voci,[53] M. Benayoun,[54] H. Briand,[54] J. Chauveau,[54] P. David,[54] Ch. de la Vaissière,[54] L. Del Buono,[54] O. Hamon,[54] F. Le Diberder,[54] Ph. Leruste,[54] J. Ocariz,[54] L. Roos,[54] J. Stark,[54] S. Versillé,[54] P. F. Manfredi,[55] V. Re,[55] V. Speziali,[55] E. D. Frank,[56] L. Gladney,[56] Q. H. Guo,[56] J. Panetta,[56] C. Angelini,[57] G. Batignani,[57] S. Bettarini,[57] M. Bondioli,[57] M. Carpinelli,[57] F. Forti,[57] M. A. Giorgi,[57] A. Lusiani,[57] F. Martinez-Vidal,[57] M. Morganti,[57] N. Neri,[57] E. Paoloni,[57] M. Rama,[57] G. Rizzo,[57] F. Sandrelli,[57] G. Simi,[57] G. Triggiani,[57] J. Walsh,[57] M. Haire,[58] D. Judd,[58] K. Paick,[58] L. Turnbull,[58] D. E. Wagoner,[58] J. Albert,[59] P. Elmer,[59] C. Lu,[59] K. T. McDonald,[59] V. Miftakov,[59] S. F. Schaffner,[59] A. J. S. Smith,[59] A. Tumanov,[59] E. W. Varnes,[59] G. Cavoto,[60] D. del Re,[60] R. Faccini,[14,60] F. Ferrarotto,[60] F. Ferroni,[60] E. Lamanna,[60] E. Leonardi,[60] M. A. Mazzoni,[60] S. Morganti,[60] G. Piredda,[60] F. Safai Tehrani,[60] M. Serra,[60] C. Voena,[60] S. Christ,[61] R. Waldi,[61] T. Adye,[62] N. De Groot,[8,62] B. Franek,[62] N. I. Geddes,[62] G. P. Gopal,[62] S. M. Xella,[62] N. Copty,[63] M. V. Purohit,[63] H. Singh,[63] F. X. Yumiceva,[63] I. Adam,[64] P. L. Anthony,[64] D. Aston,[64] K. Baird,[64] N. Berger,[64] E. Bloom,[64] A. M. Boyarski,[64] F. Bulos,[64] G. Calderini,[64] M. R. Convery,[64] D. P. Coupal,[64] D. H. Coward,[64] J. Dorfan,[64] W. Dunwoodie,[64] R. C. Field,[64] T. Glanzman,[64] G. L. Godfrey,[64] S. J. Gowdy,[64] P. Grosso,[64] T. Haas,[64] T. Himel,[64] T. Hryn'ova,[64] M. E. Huffer,[64] W. R. Innes,[64] C. P. Jessop,[64] M. H. Kelsey,[64] P. Kim,[64] M. L. Kocian,[64] U. Langenegger,[64] D. W. G. S. Leith,[64] S. Luitz,[64] V. Luth,[64] H. L. Lynch,[64] H. Marsiske,[64] S. Menke,[64] R. Messner,[64] K. C. Moffeit,[64] R. Mount,[64] D. R. Muller,[64] C. P. O'Grady,[64] V. E. Ozcan,[64] M. Perl,[64] S. Petrak,[64] H. Quinn,[64] B. N. Ratcliff,[64] S. H. Robertson,[64] L. S. Rochester,[64] A. Roodman,[64] T. Schietinger,[64] R. H. Schindler,[64] J. Schwiening,[64] V. V. Serbo,[64] A. Snyder,[64] A. Soha,[64] S. M. Spanier,[64] J. Stelzer,[64] D. Su,[64] M. K. Sullivan,[64] H. A. Tanaka,[64] J. Va'vra,[64] S. R. Wagner,[64] A. J. R. Weinstein,[64] W. J. Wisniewski,[64] D. H. Wright,[64] C. C. Young,[64] P. R. Burchat,[65] C. H. Cheng,[65] D. Kirkby,[65] T. I. Meyer,[65] C. Roat,[65] R. Henderson,[66] W. Bugg,[67] H. Cohn,[67] A. W. Weidemann,[67] J. M. Izen,[68] I. Kitayama,[68] X. C. Lou,[68] F. Bianchi,[69] M. Bona,[69] D. Gamba,[69] A. Smol,[69] L. Bosisio,[70] G. Della Ricca,[70] L. Lanceri,[70] P. Poropat,[70] G. Vuagnin,[70] R. S. Panvini,[71] C. M. Brown,[72] P. D. Jackson,[72] R. Kowalewski,[72] J. M. Roney,[72] H. R. Band,[73] E. Charles,[73] S. Dasu,[73] F. Di Lodovico,[73] A. M. Eichenbaum,[73] H. Hu,[73] J. R. Johnson,[73] R. Liu,[73] Y. Pan,[73] R. Prepost,[73] I. J. Scott,[73] S. J. Sekula,[73] J. H. von Wimmersperg-Toeller,[73] S. L. Wu,[73] Z. Yu,[73] T. M. B. Kordich,[74] and H. Neal[74]

(The *BABAR* Collaboration)

[1] *Laboratoire de Physique des Particules, F-74941 Annecy-le-Vieux, France*
[2] *Università di Bari, Dipartimento di Fisica and INFN, I-70126 Bari, Italy*
[3] *Institute of High Energy Physics, Beijing 100039, China*
[4] *University of Bergen, Inst. of Physics, N-5007 Bergen, Norway*
[5] *Lawrence Berkeley National Laboratory and University of California, Berkeley, CA 94720, USA*
[6] *University of Birmingham, Birmingham, B15 2TT, United Kingdom*
[7] *Ruhr Universität Bochum, Institut für Experimentalphysik 1, D-44780 Bochum, Germany*
[8] *University of Bristol, Bristol BS8 1TL, United Kingdom*
[9] *University of British Columbia, Vancouver, BC, Canada V6T 1Z1*
[10] *Brunel University, Uxbridge, Middlesex UB8 3PH, United Kingdom*
[11] *Budker Institute of Nuclear Physics, Novosibirsk 630090, Russia*
[12] *University of California at Irvine, Irvine, CA 92697, USA*
[13] *University of California at Los Angeles, Los Angeles, CA 90024, USA*
[14] *University of California at San Diego, La Jolla, CA 92093, USA*
[15] *University of California at Santa Barbara, Santa Barbara, CA 93106, USA*
[16] *University of California at Santa Cruz, Institute for Particle Physics, Santa Cruz, CA 95064, USA*
[17] *California Institute of Technology, Pasadena, CA 91125, USA*
[18] *University of Cincinnati, Cincinnati, OH 45221, USA*
[19] *University of Colorado, Boulder, CO 80309, USA*
[20] *Colorado State University, Fort Collins, CO 80523, USA*

[21]DAPNIA, Commissariat à l'Energie Atomique/Saclay, F-91191 Gif-sur-Yvette, France
[22]Technische Universität Dresden, Institut für Kern- und Teilchenphysik, D-01062, Dresden, Germany
[23]Ecole Polytechnique, F-91128 Palaiseau, France
[24]University of Edinburgh, Edinburgh EH9 3JZ, United Kingdom
[25]Elon University, Elon University, NC 27244-2010, USA
[26]Università di Ferrara, Dipartimento di Fisica and INFN, I-44100 Ferrara, Italy
[27]Florida A&M University, Tallahassee, FL 32307, USA
[28]Laboratori Nazionali di Frascati dell'INFN, I-00044 Frascati, Italy
[29]Università di Genova, Dipartimento di Fisica and INFN, I-16146 Genova, Italy
[30]Harvard University, Cambridge, MA 02138, USA
[31]University of Iowa, Iowa City, IA 52242, USA
[32]Iowa State University, Ames, IA 50011-3160, USA
[33]Laboratoire de l'Accélérateur Linéaire, F-91898 Orsay, France
[34]Lawrence Livermore National Laboratory, Livermore, CA 94550, USA
[35]University of Liverpool, Liverpool L69 3BX, United Kingdom
[36]University of London, Imperial College, London, SW7 2BW, United Kingdom
[37]Queen Mary, University of London, E1 4NS, United Kingdom
[38]University of London, Royal Holloway and Bedford New College, Egham, Surrey TW20 0EX, United Kingdom
[39]University of Louisville, Louisville, KY 40292, USA
[40]University of Manchester, Manchester M13 9PL, United Kingdom
[41]University of Maryland, College Park, MD 20742, USA
[42]University of Massachusetts, Amherst, MA 01003, USA
[43]Massachusetts Institute of Technology, Laboratory for Nuclear Science, Cambridge, MA 02139, USA
[44]McGill University, Montréal, QC, Canada H3A 2T8
[45]Università di Milano, Dipartimento di Fisica and INFN, I-20133 Milano, Italy
[46]University of Mississippi, University, MS 38677, USA
[47]Université de Montréal, Laboratoire René J. A. Lévesque, Montréal, QC, Canada H3C 3J7
[48]Mount Holyoke College, South Hadley, MA 01075, USA
[49]Università di Napoli Federico II, Dipartimento di Scienze Fisiche and INFN, I-80126, Napoli, Italy
[50]University of Notre Dame, Notre Dame, IN 46556, USA
[51]Oak Ridge National Laboratory, Oak Ridge, TN 37831, USA
[52]University of Oregon, Eugene, OR 97403, USA
[53]Università di Padova, Dipartimento di Fisica and INFN, I-35131 Padova, Italy
[54]Universités Paris VI et VII, Lab de Physique Nucléaire H. E., F-75252 Paris, France
[55]Università di Pavia, Dipartimento di Elettronica and INFN, I-27100 Pavia, Italy
[56]University of Pennsylvania, Philadelphia, PA 19104, USA
[57]Università di Pisa, Scuola Normale Superiore and INFN, I-56010 Pisa, Italy
[58]Prairie View A&M University, Prairie View, TX 77446, USA
[59]Princeton University, Princeton, NJ 08544, USA
[60]Università di Roma La Sapienza, Dipartimento di Fisica and INFN, I-00185 Roma, Italy
[61]Universität Rostock, D-18051 Rostock, Germany
[62]Rutherford Appleton Laboratory, Chilton, Didcot, Oxon, OX11 0QX, United Kingdom
[63]University of South Carolina, Columbia, SC 29208, USA
[64]Stanford Linear Accelerator Center, Stanford, CA 94309, USA
[65]Stanford University, Stanford, CA 94305-4060, USA
[66]TRIUMF, Vancouver, BC, Canada V6T 2A3
[67]University of Tennessee, Knoxville, TN 37996, USA
[68]University of Texas at Dallas, Richardson, TX 75083, USA
[69]Università di Torino, Dipartimento di Fiscia Sperimentale and INFN, I-10125 Torino, Italy
[70]Università di Trieste, Dipartimento di Fisica and INFN, I-34127 Trieste, Italy
[71]Vanderbilt University, Nashville, TN 37235, USA
[72]University of Victoria, Victoria, BC, Canada V8W 3P6
[73]University of Wisconsin, Madison, WI 53706, USA
[74]Yale University, New Haven, CT 06511, USA

(Dated: October 25, 2001)

We present a measurement of the time-dependent CP-violating asymmetries in neutral B decays to the $\pi^+\pi^-$ CP eigenstate, and an updated measurement of the charge asymmetry in $B^0 \to K^+\pi^-$ decays. In a sample of 33 million $\Upsilon(4S) \to B\overline{B}$ decays collected with the *BABAR* detector at the SLAC PEP-II asymmetric B Factory, we find 65^{+12}_{-11} $\pi^+\pi^-$ and 217 ± 18 $K^+\pi^-$ candidates and measure the asymmetry parameters $S_{\pi\pi} = 0.03^{+0.53}_{-0.56} \pm 0.11$, $C_{\pi\pi} = -0.25^{+0.45}_{-0.47} \pm 0.14$, and $\mathcal{A}_{K\pi} = -0.07 \pm 0.08 \pm 0.02$, where the first error is statistical and the second is systematic.

PACS numbers: 13.25.Hw, 12.15.Hh, 11.30.Er

In the Standard Model, all *CP*-violating effects arise from a single complex phase in the three-generation Cabibbo-Kobayashi-Maskawa (CKM) quark-mixing matrix [1]. One of the central questions in particle physics is whether this mechanism is sufficient to explain the pattern of *CP* violation observed in nature. Recent measurements of the parameter $\sin 2\beta$ by the *BABAR* [2] and BELLE [3] Collaborations establish that *CP* symmetry is violated in the neutral B-meson system. In addition to measuring $\sin 2\beta$ more precisely, one of the primary goals of the B-Factory experiments in the future will be to measure the remaining angles (α and γ) and sides of the Unitarity Triangle in order to further test whether the Standard Model description of *CP* violation is correct.

The study of B decays to charmless hadronic two-body final states will play an increasingly important role in our understanding of *CP* violation. In the Standard Model, the time-dependent *CP*-violating asymmetry in the reaction $B^0 \rightarrow \pi^+\pi^-$ is related to the angle α. In addition, observation of a significant rate asymmetry between $B^0 \rightarrow K^+\pi^-$ and $\overline{B}^0 \rightarrow K^-\pi^+$ decays would be evidence for direct *CP* violation, and ratios of branching fractions for various $\pi\pi$ and $K\pi$ decay modes are sensitive to the angle γ. Finally, branching fraction measurements provide critical tests of theoretical models that are needed to extract reliable information on *CP* violation from the experimental observables.

The *BABAR* Collaboration recently reported measurements of branching fractions and charge asymmetries for several charmless two-body B decays using a data set of 23 million $B\overline{B}$ pairs [4]. In this paper, using a data sample of approximately 33 million $B\overline{B}$ pairs, we report a measurement of time-dependent *CP*-violating asymmetries in neutral B decays to the $\pi^+\pi^-$ *CP* eigenstate and an updated measurement of the charge asymmetry in $B^0 \rightarrow K^+\pi^-$ decays.

The time-dependent *CP*-violating asymmetry in the decay $B^0 \rightarrow \pi^+\pi^-$ arises from interference between mixing and decay amplitudes, and interference between the tree and penguin decay amplitudes. A $B^0\overline{B}^0$ pair produced in $\Upsilon(4S)$ decay evolves in time in a coherent P-wave state until one of the two mesons decays. We reconstruct a sample of B mesons (B_{hh}) decaying to the $h^+h'^-$ final state, where h is a pion or kaon, and examine the remaining charged particles in each event to "tag" the flavor of the other B meson ($B_{\rm tag}$). The decay rate distribution f_+ (f_-) when $h^+h'^- = \pi^+\pi^-$ and $B_{\rm tag} = B^0$ ($\overline{B}^0$) is given by [5]

$$f_\pm(\Delta t) = \frac{e^{-|\Delta t|/\tau}}{4\tau}[1 \pm S_{\pi\pi}\sin(\Delta m_d \Delta t) \mp C_{\pi\pi}\cos(\Delta m_d \Delta t)], \qquad (1)$$

where τ is the B^0 lifetime, Δm_d is the $B^0\overline{B}^0$ mixing frequency, and $\Delta t = t_{hh} - t_{\rm tag}$ is the time between the B_{hh} and $B_{\rm tag}$ decays. The *CP*-violating parameters $S_{\pi\pi}$ and $C_{\pi\pi}$ are defined as

$$S_{\pi\pi} = \frac{2\,\mathcal{I}m\lambda}{1+|\lambda|^2} \quad \text{and} \quad C_{\pi\pi} = \frac{1-|\lambda|^2}{1+|\lambda|^2}. \qquad (2)$$

If the decay proceeds purely through the tree process $b \rightarrow uW^-$, the complex parameter λ is directly related to CKM matrix elements,

$$\lambda(B \rightarrow \pi^+\pi^-) = \left(\frac{V_{tb}^* V_{td}}{V_{tb} V_{td}^*}\right)\left(\frac{V_{ud}^* V_{ub}}{V_{ud} V_{ub}^*}\right), \qquad (3)$$

where we are assuming equal widths ($\Delta\Gamma_B = 0$) for the heavy and light mass eigenstates. Thus, at tree level in the Standard Model, $|\lambda| = 1$ and $\mathcal{I}m\lambda = \sin 2\alpha$, where $\alpha \equiv \arg\left[-V_{td}V_{tb}^*/V_{ud}V_{ub}^*\right]$.

Recent theoretical estimates indicate that the contribution from the gluonic penguin amplitude can be significant [6, 7, 8]. The process $b \rightarrow dg$ carries the weak phase $\arg(V_{td}^* V_{tb})$, which can modify both the magnitude and phase of λ. Thus, in general, $|\lambda| \neq 1$ and $\mathcal{I}m\lambda = |\lambda| \sin 2\alpha_{\rm eff}$, where $\alpha_{\rm eff}$ depends on the magnitudes and strong phases of the tree and penguin amplitudes. Several approaches have been proposed to obtain information on α in the presence of penguins [6, 9].

In this analysis, we extract signal and background yields for $\pi^+\pi^-$, $K^+\pi^-$, and K^+K^- decays [10], and the amplitudes of the $\pi\pi$ sine ($S_{\pi\pi}$) and cosine ($C_{\pi\pi}$) oscillation terms simultaneously from an unbinned maximum likelihood fit. We parameterize the $K\pi$ component in terms of the total yield and the *CP*-violating charge asymmetry

$$\mathcal{A}_{K\pi} \equiv \frac{N_{K^-\pi^+} - N_{K^+\pi^-}}{N_{K^-\pi^+} + N_{K^+\pi^-}}. \qquad (4)$$

The data sample used in this analysis consists of $33.7\,\mathrm{fb}^{-1}$ collected with the *BABAR* detector at the SLAC PEP-II storage ring between October 1999 and June 2001. The PEP-II facility operates nominally at the $\Upsilon(4S)$ resonance, providing collisions of 9.0 GeV electrons on 3.1 GeV positrons. The data set includes $30.4\,\mathrm{fb}^{-1}$ collected in this configuration (on-resonance) and $3.3\,\mathrm{fb}^{-1}$ collected below the $B\overline{B}$ threshold (off-resonance) that are used for continuum background studies.

A detailed description of the *BABAR* detector is presented in Ref. [11]. Charged particle (track) momenta are measured in a tracking system consisting of a 5-layer double-sided silicon vertex tracker (SVT) and a 40-layer drift chamber (DCH) filled with a gas mixture of helium and isobutane. The SVT and DCH operate within a 1.5 T superconducting solenoidal magnet. The typical decay vertex resolution for fully reconstructed B decays is approximately $65\,\mu$m along the center-of-mass (CM) boost direction. Photons are detected in an electromagnetic calorimeter (EMC) consisting of 6580 CsI(Tl) crystals arranged in barrel and forward endcap subdetectors.

The flux return for the solenoid is composed of multiple layers of iron and resistive plate chambers for the identification of muons and long-lived neutral hadrons.

Tracks from the B_{hh} decay are identified as pions or kaons by the Cherenkov angle θ_c measured with a detector of internally reflected Cherenkov light (DIRC). The typical separation between pions and kaons varies from 8σ at $2\,\mathrm{GeV}/c$ to 2.5σ at $4\,\mathrm{GeV}/c$, where σ is the average resolution on θ_c. Lower momentum kaons used in B flavor tagging are identified with a combination of θ_c (for momenta down to $0.7\,\mathrm{GeV}/c$) and measurements of ionization energy loss dE/dx in the DCH and SVT.

Hadronic events are selected based on track multiplicity and event topology. We require at least three tracks in the laboratory polar angle region $0.41 < \theta_{\mathrm{lab}} < 2.54$ satisfying the following requirements: transverse momentum greater than $100\,\mathrm{MeV}/c$, at least 12 DCH hits, and originating from the interaction point within 10 cm in z and 1.5 cm in r–φ [12]. Residual two-prong events from the reaction $e^+e^- \to l^+l^-$ $(l = e, \mu, \tau)$ are suppressed by requiring the ratio of Fox-Wolfram moments H_2/H_0 [13] to be less than 0.95 and the sphericity [14] of the event to be greater than 0.01.

Candidate B_{hh} decays are reconstructed from pairs of oppositely-charged tracks forming a good quality vertex, where the B_{hh} four-vector is calculated assuming the pion mass for both tracks. We require each track to have an associated θ_c measurement with a minimum of six Cherenkov photons above background, where the average is approximately 30 for both pions and kaons. Protons are rejected based on θ_c and electrons are rejected based on dE/dx, shower shape in the EMC, and the ratio of shower energy and track momentum. Background from the reaction $e^+e^- \to q\bar{q}$ $(q = u, d, s, c)$ is suppressed by removing jet-like events from the sample: we define the CM angle θ_S between the sphericity axes of the B candidate and the remaining tracks and photons in the event, and require $|\cos\theta_S| < 0.8$, which removes 83% of the background. The total efficiency on signal events for all of the above selection is approximately 38%.

We define a beam-energy substituted mass $m_{\mathrm{ES}} = \sqrt{E_{\mathrm{b}}^2 - \mathbf{p}_B^2}$. The candidate energy is defined as $E_{\mathrm{b}} = (s/2 + \mathbf{p}_i \cdot \mathbf{p}_B)/E_i$, where $\sqrt{s}$ and E_i are the total energies of the e^+e^- system in the CM and laboratory frames, respectively, and $\mathbf{p}_i$ and $\mathbf{p}_B$ are the momentum vectors in the laboratory frame of the e^+e^- system and the B_{hh} candidate, respectively. Signal events are Gaussian distributed in m_{ES} with a mean near the B mass and a resolution of $2.6\,\mathrm{MeV}/c^2$, dominated by the beam energy spread. The background shape is parameterized by a threshold function [15] with a fixed endpoint given by the average beam energy.

We define a second kinematic variable ΔE as the difference between the energy of the B_{hh} candidate in the CM frame and $\sqrt{s}/2$. The ΔE distribution is peaked near zero for $\pi^+\pi^-$ decays. For decays with one (two) kaons, the distribution is shifted relative to $\pi\pi$ on average by $-45\,\mathrm{MeV}$ ($-91\,\mathrm{MeV}$), respectively, where the exact separation depends on the laboratory momentum of the kaon(s). The resolution on ΔE for signal decays is approximately 26 MeV. The background is parameterized by a quadratic function.

Candidate $h^+h'^-$ pairs selected in the region $5.2 < m_{\mathrm{ES}} < 5.3\,\mathrm{GeV}/c^2$ and $|\Delta E| < 0.15\,\mathrm{GeV}$ are used to extract yields and CP-violating asymmetries with an unbinned maximum likelihood fit. The total number of events in the fit region satisfying all of the above criteria is 9741. A sideband region, defined as $5.20 < m_{\mathrm{ES}} < 5.26\,\mathrm{GeV}/c^2$ and $|\Delta E| < 0.42\,\mathrm{GeV}$, is used to extract various background parameters.

The analysis method combines the techniques used to measure charmless two-body branching fractions [4] and $\sin 2\beta$ [2]. The primary issues in this analysis are determination of the B_{tag} flavor, measurement of the distance Δz between the B_{hh} and B_{tag} decay vertices, discrimination of signal from background, identification of pions and kaons, and extraction of yields and CP asymmetries.

To determine the flavor of the B_{tag} meson we use the same B-tagging algorithm used in the $\sin 2\beta$ and B^0–$\overline{B}^0$ mixing [16] analyses. The algorithm relies on the correlation between the flavor of the b quark and the charge of the remaining tracks in the event after removal of the B_{hh} candidate. We define five mutually exclusive tagging categories: `Lepton`, `Kaon`, `NT1`, `NT2`, and `Untagged`. `Lepton` tags rely on primary electrons and muons from semileptonic B decays, while `Kaon` tags exploit the correlation in the process $b \to c \to s$ between the net kaon charge and the charge of the b quark. The `NT1` and `NT2` categories are derived from a neural network that is sensitive to charge correlations between the parent B and unidentified leptons and kaons, soft pions, or the charge and momentum of the track with the highest CM momentum. The addition of `Untagged` events improves the signal yield estimates and provides a larger sample for determining background shape parameters directly in the maximum likelihood fit.

The quality of tagging is expressed in terms of the effective efficiency $Q = \sum_i \epsilon_i D_i^2$, where ϵ_i is the fraction of events tagged in category i and the dilution $D_i = 1 - 2w_i$ is related to the mistag fraction w_i. The statistical errors on $S_{\pi\pi}$ and $C_{\pi\pi}$ are proportional to $1/\sqrt{Q}$. Table I summarizes the tagging performance in a data sample B_{flav} of fully reconstructed neutral B decays into $D^{(*)-}h^+$ $(h^+ = \pi^+, \rho^+, a_1^+)$ and $J/\psi K^{*0}$ $(K^{*0} \to K^+\pi^-)$ flavor eigenstates We use the same tagging efficiencies and dilutions for signal $\pi\pi$, $K\pi$, and KK decays. Separate background tagging efficiencies for each species are obtained from a fit to the $h^+h'^-$ on-resonance sideband data and reported in Table II.

The time difference Δt is obtained from the measured distance between the z position of the B_{hh} and B_{tag} decay vertices and the known boost of the e^+e^- system.

TABLE I: Tagging efficiency ϵ, average dilution $D = 1/2\left(D_{B^0} + D_{\overline{B}^0}\right)$, dilution difference $\Delta D = D_{B^0} - D_{\overline{B}^0}$, and effective tagging efficiency Q for signal events in each tagging category.

Category	$\epsilon\,(\%)$	$D\,(\%)$	$\Delta D\,(\%)$	$Q\,(\%)$
`Lepton`	11.0 ± 0.3	82.3 ± 2.7	-2.1 ± 4.5	7.5 ± 0.5
`Kaon`	35.8 ± 0.5	64.8 ± 2.0	3.5 ± 3.1	15.0 ± 1.0
`NT1`	8.0 ± 0.3	55.6 ± 4.2	-12.1 ± 6.7	2.5 ± 0.4
`NT2`	13.9 ± 0.4	30.2 ± 3.8	9.0 ± 5.7	1.3 ± 0.3
`Untagged`	31.3 ± 0.5	–	–	–
Total Q				26.3 ± 1.2

TABLE II: Tagging efficiencies (%) for background events in each species.

Category	$\epsilon(\pi\pi)$	$\epsilon(K\pi)$	$\epsilon(KK)$
`Lepton`	1.0 ± 0.1	1.0 ± 0.1	1.5 ± 0.2
`Kaon`	26.0 ± 0.4	33.1 ± 0.6	23.5 ± 0.7
`NT1`	6.6 ± 0.2	5.4 ± 0.3	6.9 ± 0.4
`NT2`	17.6 ± 0.4	15.3 ± 0.5	19.7 ± 0.6
`Untagged`	48.9 ± 0.7	45.2 ± 0.6	48.3 ± 0.8

The z position of the $B_{\rm tag}$ vertex is determined with an iterative procedure that removes tracks with a large contribution to the total χ^2 [2, 16]. An additional constraint is constructed from the three-momentum and vertex position of the B_{hh} candidate, and the average e^+e^- interaction point and boost. The typical Δz resolution is $180\,\mu$m. We require $|\Delta t| < 17\,$ps and $0.3 < \sigma_{\Delta t} < 3.0\,$ps, where $\sigma_{\Delta t}$ is the error from the vertex fit. The resolution function for signal candidates is a sum of three Gaussians, identical to the one described in Ref. [2], with parameters determined from a fit to the $B_{\rm flav}$ sample (including events in all five tagging categories). The background resolution function is parameterized as the sum of three Gaussians, with the parameters determined from a fit to the $h^+h'^-$ on-resonance sideband data.

The data sample used in the fit contains 97% background, mostly due to random combinations of tracks produced in $e^+e^- \to q\bar{q}$ events. Discrimination of signal from background in the maximum likelihood fit is enhanced by the use of a Fisher discriminant $\mathcal{F}$ [4]. The discriminating variables are constructed from the scalar sum of the CM momenta of all tracks and photons (excluding tracks from the B_{hh} candidate) entering nine two-sided 10-degree concentric cones centered on the thrust axis of the B_{hh} candidate. The distribution of $\mathcal{F}$ for signal events is parameterized as a single Gaussian, with parameters determined from Monte Carlo simulated decays and validated with $B^- \to D^0\pi^-$ decays reconstructed in data. The background shape is parameterized as the sum of two Gaussians, with parameters determined directly in the maximum likelihood fit.

Identification of $h^+h'^-$ tracks as pions or kaons is accomplished with the Cherenkov angle measurement from the DIRC. We construct Gaussian probability density functions (PDFs) from the difference between measured and expected values of θ_c for the pion or kaon hypothesis, normalized by the resolution. The DIRC performance is parameterized using a sample of $D^{*+} \to D^0\pi^+$, $D^0 \to K^-\pi^+$ decays reconstructed in data. Within the statistical precision of the control sample (approximately 10^5 events), we find similar response for positively and negatively charged tracks and use a single parameterization for both.

We use an unbinned extended maximum likelihood fit to extract yields and *CP* parameters from the B_{hh} sample. The likelihood for candidate j tagged in category c is obtained by summing the product of event yield n_i, tagging efficiency $\epsilon_{i,c}$, and probability $\mathcal{P}_{i,c}$ over the eight possible signal and background hypotheses i (referring to $\pi\pi$, $K^+\pi^-$, $K^-\pi^+$, and KK decays),

$$\mathcal{L}_c = \exp\left(-\sum_i n_i\epsilon_{i,c}\right)\prod_j\left[\sum_i n_i\epsilon_{i,c}\mathcal{P}_{i,c}(\vec{x}_j;\vec{\alpha}_i)\right]. \tag{5}$$

For the $K^\mp\pi^\pm$ hypotheses, the yield is parameterized as $n_i = N_{K\pi}\left(1 \pm \mathcal{A}_{K\pi}\right)/2$, where $N_{K\pi} = N_{K^-\pi^+} + N_{K^+\pi^-}$. We fix the tagging efficiencies ϵ_i to the values in Tables I and II. The probabilities $\mathcal{P}_{i,c}$ are evaluated as the product of PDFs for each of the independent variables $\vec{x}_j = \{m_{\rm ES}, \Delta E, \mathcal{F}, \theta_c^+, \theta_c^-, \Delta t\}$, where θ_c^+ and θ_c^- are the Cherenkov angles for the positively and negatively charged tracks. The total likelihood $\mathcal{L}$ is the product of likelihoods for each tagging category and the free parameters are determined by minimizing the quantity $\ln\mathcal{L}$.

The Δt PDF for signal $\pi^+\pi^-$ decays is given by Eq. 1, modified to include the dilution and dilution difference for each tagging category, and convolved with the signal resolution function. The Δt PDF for signal $K\pi$ events takes into account B^0–$\overline{B}^0$ mixing, depending on the charge of the kaon and the flavor of $B_{\rm tag}$. We parameterize $B^0 \to K^+K^-$ decays as an exponential convolved with the resolution function.

There are 18 free parameters in the fit. In addition to the *CP*-violating parameters $S_{\pi\pi}$, $C_{\pi\pi}$, and $\mathcal{A}_{K\pi}$, the fit determines signal and background yields (six parameters), the background $K\pi$ charge asymmetry, and eight parameters describing the background shapes in $m_{\rm ES}$, ΔE, and $\mathcal{F}$. We fix τ and Δm_d to the world-average values [17].

In a sample of 33 million $B\overline{B}$ pairs we find 65^{+12}_{-11} $\pi\pi$, 217 ± 18 $K\pi$, and $4.3^{+6.3}_{-4.3}$ KK events. These yields are consistent with the branching fractions reported in

TABLE III: Central values and 90% C.L. intervals for $S_{\pi\pi}$, $C_{\pi\pi}$, and $\mathcal{A}_{K\pi}$ from the maximum likelihood fit.

Parameter	Central Value	90% C.L. Interval
$S_{\pi\pi}$	$0.03^{+0.53}_{-0.56} \pm 0.11$	$[-0.89, +0.85]$
$C_{\pi\pi}$	$-0.25^{+0.45}_{-0.47} \pm 0.14$	$[-1.0, +0.47]$
$\mathcal{A}_{K\pi}$	$-0.07 \pm 0.08 \pm 0.02$	$[-0.21, +0.07]$

Ref. [4], as well as measurements from other experiments [18, 19]. The results for *CP*-violating asymmetries are summarized in Table III. Statistical errors correspond to unit change in $\chi^2 \equiv -2\ln(\mathcal{L})$. For each parameter, we also calculate the 90% confidence level (C.L.) interval corresponding to a change in χ^2 of 2.69, and taking into account the systematic error. The correlation between $S_{\pi\pi}$ and $C_{\pi\pi}$ is -21%, while $\mathcal{A}_{K\pi}$ is uncorrelated with either $S_{\pi\pi}$ or $C_{\pi\pi}$.

Figure 1 shows distributions of $m_{\rm ES}$ and ΔE for events enhanced in signal decays based on likelihood ratios. We define $\mathcal{R}_{\rm sig} = \sum_s n_s\mathcal{P}_s/\sum_i n_i\mathcal{P}_i$ and $\mathcal{R}_k = n_k\mathcal{P}_k/\sum_s n_s\mathcal{P}_s$, where $\sum_s$ ($\sum_i$) indicates a sum over signal (all) hypotheses, and $\mathcal{P}_k$ indicates the probability for signal hypothesis k. The probabilities include the PDFs for θ_c, $\mathcal{F}$, and $m_{\rm ES}$ (ΔE) when plotting ΔE ($m_{\rm ES}$). The selection is defined by optimizing the signal significance with respect to $\mathcal{R}_{\rm sig}$ and $\mathcal{R}_k$. The solid curve in each plot represents the fit projection after correcting for the efficiency of the additional selection (approximately 55% for $\pi\pi$ and 85% for $K\pi$).

Figure 2 shows the Δt distributions and the asymmetry $\mathcal{A}_{\pi\pi}(\Delta t) = (N_{B^0}(\Delta t) - N_{\overline{B}^0}(\Delta t))/(N_{B^0}(\Delta t) + N_{\overline{B}^0}(\Delta t))$ for tagged events enhanced in signal $\pi\pi$ decays. The selection procedure is the same as Fig. 1, with the likelihoods defined including the PDFs for θ_c, $\mathcal{F}$, $m_{\rm ES}$, and ΔE. Approximately 24 $\pi\pi$, 22 $q\bar{q}$, and 5 $K\pi$ events satisfy the selection.

Systematic uncertainties on $S_{\pi\pi}$, $C_{\pi\pi}$, and $\mathcal{A}_{K\pi}$ arise primarily from imperfect knowledge of the PDF shapes and uncertainties on tagging efficiencies, dilutions, τ, and Δm_d. The total systematic error is calculated as the sum in quadrature of the individual uncertainties. The error on $\mathcal{A}_{K\pi}$ is dominated by uncertainty in the mean of the ΔE PDF (0.01) and possible charge bias in track and θ_c reconstruction (0.01) [20]. Errors on $S_{\pi\pi}$ and $C_{\pi\pi}$ are dominated by the parameterization of Δt resolution for signal and background (≈ 0.07 for $S_{\pi\pi}$, ≈ 0.03 for $C_{\pi\pi}$), tagging (0.05), and, for $C_{\pi\pi}$ only, the mean of the ΔE PDF (0.1).

Extensive studies were performed to validate the fit technique. A large ensemble of Monte Carlo pseudo-experiments was generated from the nominal PDFs with the statistics observed in the full data set. Parameter errors and the maximum value of the likelihood obtained in the data fit are all consistent with expectations based on these pseudo-experiments, and all free parameters are unbiased. We have checked that consistent results are obtained when separating events by $B_{\rm tag}$ flavor. As a

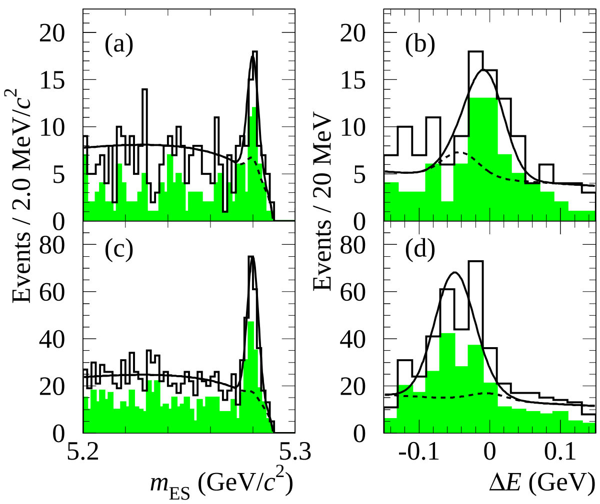

FIG. 1: Distributions of $m_{\rm ES}$ and ΔE (unshaded histograms) for events enhanced in signal (a), (b) $\pi\pi$ and (c), (d) $K\pi$ decays based on the likelihood ratio selection described in the text. Solid curves represent projections of the maximum likelihood fit result after accounting for the efficiency of the additional selection, while dashed curves represent $q\bar{q}$ and $\pi\pi \leftrightarrow K\pi$ cross-feed background. Shaded histograms show the subset of events that are tagged.

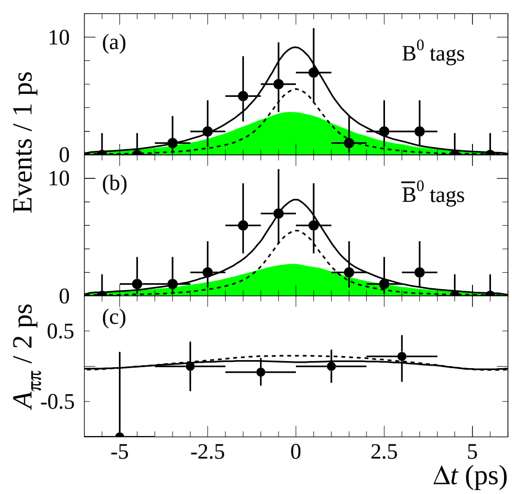

FIG. 2: Distributions of Δt for events enhanced in signal $\pi\pi$ decays based on the likelihood ratio selection described in the text. Figures (a) and (b) show events (points with errors) with $B_{\rm tag} = B^0$ or $\overline{B}^0$. Solid curves represent projections of the maximum likelihood fit, dashed curves represent the sum of $q\bar{q}$ and $K\pi$ background events, and the shaded region represents the contribution from signal $\pi\pi$ events. Figure (c) shows $\mathcal{A}_{\pi\pi}(\Delta t)$ for data (points with errors), as well as fit projections for signal and background events (solid curve), and signal events only (dashed curve).

validation of the Δt parameterization in data, we fit the full data set to simultaneously extract yields, background parameters, τ, Δm_d, $S_{\pi\pi}$, and $C_{\pi\pi}$. We find $\tau = (1.52 \pm 0.12)\,\mathrm{ps}$ and $\Delta m_d = (0.54 \pm 0.09)\hbar\,\mathrm{ps}^{-1}$, and all other parameters are consistent with the nominal fit.

In summary, we have presented a measurement of time-dependent *CP*-violating asymmetries in $B^0 \to \pi^+\pi^-$ decays and an updated measurement of the charge asymmetry $\mathcal{A}_{K\pi}$. The latter is consistent with our previous result reported in Ref. [4], as well as results from other experiments [21, 22]. We observe no evidence for direct *CP* violation in the $K\pi$ mode and determine a 90% C.L. interval excluding a significant part of the allowed region. Although the current measurements of $S_{\pi\pi}$ and $C_{\pi\pi}$ do not significantly constrain the Unitarity Triangle, with the addition of more data and further improvements in detector performance and analysis techniques, future results will yield important information about *CP* violation in the *B*-meson system.

We are grateful for the excellent luminosity and machine conditions provided by our PEP-II colleagues. The collaborating institutions wish to thank SLAC for its support and kind hospitality. This work is supported by DOE and NSF (USA), NSERC (Canada), IHEP (China), CEA and CNRS-IN2P3 (France), BMBF (Germany), INFN (Italy), NFR (Norway), MIST (Russia), and PPARC (United Kingdom). Individuals have received support from the Swiss NSF, A. P. Sloan Foundation, Research Corporation, and Alexander von Humboldt Foundation.

* Also with Università di Perugia, Perugia, Italy
† Also with Università della Basilicata, Potenza, Italy

[1] N. Cabibbo, Phys. Rev. Lett. **10**, 531 (1963); M. Kobayashi and T. Maskawa, Prog. Th. Phys. **49**, 652 (1973).
[2] *BABAR* Collaboration, B. Aubert *et al.*, Phys. Rev. Lett. **87**, 091801 (2001).
[3] BELLE Collaboration, K. Abe *et al.*, Phys. Rev. Lett. **87**, 091802 (2001).
[4] *BABAR* Collaboration, B. Aubert *et al.*, Phys. Rev. Lett. **87**, 151802 (2001).
[5] For a general review of the formalism see Y. Nir and H. Quinn, Ann. Rev. Nucl. Part. Sci. **42**, 211 (1992).
[6] M. Beneke, G. Buchalla, M. Neubert, and C.T. Sachrajda, Nucl. Phys. B **606**, 245 (2001).
[7] Y.Y. Keum, H-n. Li, and A.I. Sanda, Phys. Rev. D **63**, 054008 (2001).
[8] M. Ciuchini *et al.*, Phys. Lett. B **515**, 33 (2001).
[9] M. Gronau and D. London, Phys. Rev. Lett. **65**, 3381 (1990); Y. Grossman and H.R. Quinn, Phys. Rev. D **58**, 017504 (1998); J. Charles, Phys. Rev. D **59**, 054007 (1999); M. Gronau, D. London, N. Sinha, and R. Sinha, Phys. Lett. B **514**, 315 (2001).
[10] When only one charge mode is given, conjugate decay modes are implied.
[11] *BABAR* Collaboration, B. Aubert *et al.*, *BABAR*-PUB-01/08, to appear in Nucl. Instrum. Methods.
[12] The unit vector $\hat{z}$ is aligned along the detector axis in the electron beam direction.
[13] G.C. Fox and S. Wolfram, Phys. Rev. Lett. **41**, 1581 (1978).
[14] S.L. Wu, Phys. Rep. **107**, 59 (1984).
[15] ARGUS Collaboration, H. Albrecht *et al.*, Z. Phys. C **48**, 543 (1990).
[16] *BABAR* Collaboration, B. Aubert *et al.*, hep-ex/0107036, submitted to the 20^{th} International Symposium on Lepton and Photon Interactions at High Energies, Rome, Italy (2001).
[17] Particle Data Group, D.E. Groom *et al.*, Eur. Phys. Jour. C **15**, 1 (2000).
[18] CLEO Collaboration, D. Cronin-Hennessey *et al.*, Phys. Rev. Lett. **85**, 515 (2000).
[19] BELLE Collaboration, K. Abe *et al.*, Phys. Rev. Lett. **87**, 101801 (2001).
[20] *BABAR* Collaboration, B. Aubert *et al.*, *BABAR*-PUB-01/23, hep-ex/0109006, to be submitted to Phys. Rev. D
[21] CLEO Collaboration, S. Chen *et al.*, Phys. Rev. Lett. **85**, 525 (2000).
[22] BELLE Collaboration, K. Abe *et al.*, Phys. Rev. D **64**, 071101 (2001).